J|A|C|S
ARTICLES
Published on Web 03/21/2002

Investigation of the Electron-Transfer Mechanism by Cross-Linking between Zn-substituted Myoglobin and Cytochrome b_5

Yoshiaki Furukawa, Fumihiro Matsuda, Koichiro Ishimori, and Isao Morishima*

Contribution from the Department of Molecular Engineering, Graduate School of Engineering, Kyoto University, Kyoto 606-8501, Japan

Received September 28, 2001

Abstract: We have investigated the photoinduced electron transfer (ET) in the 1:1 cross-linked complex (CL-ZnMb/b_5) formed by a cross-linking reagent, EDC, between Zn-substituted myoglobin (ZnMb) and cytochrome b_5 (Cytb_5) to reveal the mechanism of the *inter*-protein ET reactions under the condition of multiple encounter complexes. A variety of the ZnMb−Cytb_5 orientations was suggested because of failure to identify the single and specific cross-linking site on Cytb_5 by the peptide-mapping analysis using mass spectrometry. In CL-ZnMb/b_5, a laser pulse generates the triplet excited state of the ZnMb domain (^{3}ZnMb*), which can transfer one electron to the Cytb_5 domain. The decay kinetics of ^{3}ZnMb* in CL-ZnMb/b_5 consists of a facile power-law ET phase to Cytb_5 domain (∼30%) and a slower single-exponential phase (∼70%). The application of the Marcus equation to this power-law phase indicates that CL-ZnMb/b_5 has a variety of ZnMb−Cytb_5 orientations for the facile ET in which the distance between the redox centers (D−A distance) is distributed over 13−20 Å. The single-exponential phase in the ^{3}ZnMb* decay kinetics of CL-ZnMb/b_5 is similar to the intrinsic decay of ^{3}ZnMb* in its rate constant, 65 s^{-1}. This implies that the ET is impeded in about 70% of the total ZnMb−Cytb_5 orientations due to the D−A distance larger than 20 Å. Combined with the results of the Brownian dynamics simulations for the encounter complexes, the overall bimolecular ET rate, k_{app}, can be reproduced by the sum of the ET rates for the minor encounter complexes of which D−A distance is less than 20 Å. On the other hand, the encounter complexes with longer D−A distance, which are the majority of the encounter complexes between ZnMb and Cytb_5, have little contribution to the overall bimolecular ET rate. These observations experimentally demonstrate that ZnMb forms a variety of encounter complexes with Cytb_5, among which a minor set of the complexes with the shorter D−A distance (<∼20 Å) regulates the overall bimolecular ET between the proteins.

Introduction

Many biological redox processes depend on the electron transfer (ET) from one protein to its partner protein. Since a protein recognizes its partner and forms a complex to transfer electrons in the *inter*-protein ET reactions, much attention has been paid to the relationship between the formation of the protein−protein complex and its ET reaction.[1−4] Recent advances in X-ray crystallography have resulted in increasing numbers of three-dimensional structures of ET complexes at the atomic-level.[5−8] As seen in the crystal structure of the cytochrome *c*−cytochrome *c* peroxidase complex,[5] for instance, the interprotein ET reaction is considered to be regulated by the specific interactions between the proteins. That is, the electrostatic interaction between uniquely distributed charged patches on each protein surface guides them to a specific orientation of the reactant complex for the facile ET. Important insights have resulted from the cocrystallization of redox partners, but the crystallographic data provide only static structures for the complex, and such crystalline complexes might represent only one of a set of the productive orientations.[9]

Alternatively, recent computer simulations[10,11] have shown that redox protein molecules can form a complex with a variety of orientations, and the ET reaction is achieved in these encounter complexes, rather than in the single dominant complex, suggesting that, among a set of the plausible protein−protein orientations formed in solution, a minority of orientations might regulate the interprotein ET reactions.[10,11] However, there are few studies to experimentally show the complex formation

* To whom correspondence should be addressed. Telephone: +81-75-753-5921. Fax: +81-75-751-7611. E-mail: morisima@mds.moleng.kyoto-u.ac.jp.

(1) McLendon, G.; Hake, R. *Chem. Rev.* **1992**, *92*, 481−490.
(2) Mauk, A. G.; Mauk, M. R.; Moore, G. R.; Northrup, S. H. *J. Bioenerg. Biomembr.* **1995**, *27*, 311−330.
(3) Durham, B.; Fairris, J. L.; McLean, M.; Millet, F.; Scott, J. R.; Sligar, S. G.; Willie, A. *J. Bioenerg. Biomembr.* **1995**, *27*, 331−340.
(4) Nocek, J. M.; Zhou, J. S.; Forest, S. D.; Priyadarshy, S.; Beratan, D. N.; Onuchic, J. N.; Hoffman, B. M. *Chem. Rev.* **1996**, *96*, 2459−2489.
(5) Pelletier, H.; Kraut, J. *Science* **1992**, *258*, 1748−1755.
(6) Sevrioukova, I. F.; Li, H.; Zhang, H.; Peterson, J. A.; Poulos, T. L. *Proc. Natl. Acad. Sci. U.S.A.* **1999**, *96*, 1863−1868.
(7) Kurisu, G.; Kusunoki, M.; Katoh, E.; Yamazaki, T.; Teshima, K.; Onda, Y.; Kimata-Ariga, Y.; Hase, T. *Nat. Struct. Biol.* **2001**, *8*, 117−121.
(8) Muller, J. J.; Lapko, A.; Bourenkov, G.; Ruckpaul, K.; Heinemann, U. *J. Biol. Chem.* **2001**, *276*, 2786−2789.
(9) Zhang, Z.; Huang, L.; Shulmeister, V. M.; Chi, Y.; Kim, K. K.; Hung, L.; Crofts, A. R.; Berry, E. A.; Kim, S. *Nature* **1998**, *392*, 677−684.
(10) Gabdoulline, R. R.; Wade, R. C. *J. Mol. Recogn.* **1999**, *12*, 226−234.
(11) Northrup, S. H.; Boles, J. O.; Reynolds, J. C. L. *Science* **1988**, *241*, 67−70.

10.1021/ja0171916 CCC: $22.00

with a variety of complex configurations and describe the redox reactivity in each configuration, which is necessary for understanding the mechanism of interprotein ET reactions under the multiple configurations. Indeed, Nocek et al.[12] have performed the Brownian dynamics simulations between myoglobin (Mb) and cytochrome b_5 (Cytb_5) and suggested that Mb has a broad reactive surface in the ET reaction with Cytb_5 which encompasses the hemisphere of Mb including the exposed heme edge. On the basis of this simulation, Liang et al.[13] have substituted Zn−porphyrin for heme in Mb (ZnMb) to enable the photoinduced ET and perturbed the electrostatic potential on the Mb surface by esterification of the surface-exposed heme propionates. They observed the 100-fold enhancement of the photoinduced ET rate constant *without* altering the net binding constant. In their interpretation, neutralization of the propionates enhances formation of the minor encounter complexes with the fast ET rate, without changing its binding constant, but has a minimal influence on the majority set of the less-reactive conformers, which continue to dominate the overall binding. The ET reaction in the ZnMb−Cytb_5 complex is, therefore, associated with a small minority of the highly reactive conformations, while the binding constant is determined by conformations with very small ET rate constants. Although these observations strongly suggest the predominant role of the minor and highly reactive encounter complexes in the ET reaction from ZnMb to Cytb_5, the contribution of these encounter complexes to the overall ET rate has not yet been quantitatively examined.

One of the difficulties to quantitatively discuss the contribution of the specific encounter complex to the overall ET reaction can be attributed to the relatively low binding affinity between the redox proteins. In the case of Mb and Cytb_5, the overall binding constant has been reported to be as much as 10^2 M^{-1} [13] under moderate ionic strength (∼50 mM), meaning that the complex is approximately up to only 0.2% of the total protein concentrations in the usual kinetic experiments (∼20 μM protein). In addition to the low affinity between the two proteins, the proposed multiplicity in the binding states, as mentioned above, has made it difficult to elucidate the mechanism of the complex formation for the ET reaction. To gain an insight into a variety of the encounter complexes with low binding affinity in the ET process between Mb and Cytb_5, we have examined here the ET reaction within the persistent diprotein complex, which is reinforced by noninvasive cross-links between Mb and Cytb_5. Cross-linking has been used as a method to trap the orientation of proteins in such encounter complexes.[14−19] 1-Ethyl-3-[3-(dimethylamino)propyl]carbodiimide (EDC) was chosen here as the cross-linking agent, because the ^{1}H NMR[20] and the computer graphics modeling[12] of the encounter complexes predict a number of salt linkages between ϵ-amino groups on the surface of Mb and carboxylate groups on the surface of Cytb_5, and EDC is known to catalyze the formation of amide bonds between interacting groups of this type.[21]

To evaluate the ET rate constants in the encounter complexes between Mb and Cytb_5, we utilized in this study laser-flash photolysis and examined the photoinduced ET reactions for the cross-linked complex between ZnMb and Cytb_5 (CL-ZnMb/b_5). Replacement of Fe(II) by Zn(II) does not perturb the structure of many five-coordinated hemoproteins,[22−24] and the triplet-excited state of Zn−porphyrin is long-lived and suitable for various kinetic studies. Along with the docking simulation using the Brownian dynamics algorithm, the ET kinetics in CL-ZnMb/b_5 would provide us with the effects of the multiple conformations in the protein−protein encounter complexes on the *inter*-protein ET mechanism.

Experimental Procedures

Protein Preparation. Cytochrome b_5 (Cytb_5) was prepared as reported previously.[25] *Escherichia coli* TB-1 cells containing plasmid, pUC13, harboring the gene for the soluble heme-containing domain of rat hepatic Cytb_5 were grown in 2xTY culture in shaken flasks overnight. The final purified Cytb_5 gave a single band on SDS polyacrylamide gels and an A_{413}/A_{280} ratio of 5.8, and was stored at −80 °C.

Horse heart myoglobin (Mb) was purchased from Sigma Chemical Co. To prepare the apo-form of Mb, heme was removed from Mb by the acid−butanone method.[26] After the pH of the Mb solution was lowered to ca. 3.0, an equivolume of 2-butanone was added to the solution to extract heme. The extraction was repeated twice, and the aqueous apoprotein solution (∼ 20 mL) was dialyzed against 2 L of 20 mM borate−NaOH buffer, pH 10, for overnight.

The apoprotein solution was maintained at 4 °C in the reconstitution of Zn−mesoporphyrin IX diacid (ZnMP). Approximately 5 mg of ZnMP (Sigma Chemical Co.) was dissolved in 0.5 mL of dimethyl formamide and was added dropwise to the apoMb solution (ca. 20 mL) with gentle stirring. The reaction mixture was stirred overnight in the dark at 4 °C. The total volume of the crude ZnMP-substituted Mb (ZnMb) solution was reduced to ca. 5 mL by using Centrifugal Filter Device (Millipore), and the concentrated ZnMb solution was loaded onto the PD-10 gel filtration column (Amersham Pharmacia Biotech), which was preequilibrated with 10 mM Tris-HCl, pH 9.2, to remove excess ZnMP. The eluted crude ZnMb was further purified by a HiTrap Q anion-exchange column fitted to the Pharmacia FPLC system. The samples were loaded on the column equilibrated with 10 mM Tris-HCl, pH 9.2, and eluted with a linear gradient of 50 mM Tris-HCl, 1 M NaCl, and pH 8.0. The sample purity was confirmed by an A_{414}/A_{280} ratio of >16 as previously reported.[27]

Cross-Linking between ZnMb and Cytb_5. Previous studies have suggested that the interaction between ZnMb and Cytb_5 is dominantly electrostatic.[12,20,28] To facilitate the association and the cross-link between ZnMb and Cytb_5, we performed the cross-linking experiments under low ionic strength, 1 mM Na-P$_i$, pH 6.0.[29] Incubation of the reaction mixture containing 300 μM ZnMb and 300 μM Cytb_5 was started by addition of sulfo-NHS (*N*-hydroxysulfosuccinimide) and EDC

(12) Nocek, J. M.; Sishta, B. P.; Cameron, J. C.; Mauk, A. G.; Hoffman, B. M. *J. Am. Chem. Soc.* **1997**, *119*, 2146−2155.
(13) Liang, Z.; Nocek, J. M.; Kurnikov, I. V.; Beratan, D. N.; Hoffman, B. M. *J. Am. Chem. Soc.* **2000**, *122*, 3552−3553.
(14) Zhou, J. S.; Brothers II, H. M.; Neddersen, J. P.; Peerey, L. M.; Cotton, T. M.; Kostic, N. M. *Bioconjug. Chem.* **1992**, *3*, 382−390.
(15) Alleyne, T. A.; Wilson, M. T.; Antonini, G.; Malatesta, F.; Vallone, B.; Sarti, P.; Brunori, M. *Biochem. J.* **1992**, *287*, 951−956.
(16) Qin, L.; Kostic, N. M. *Biochemistry* **1993**, *32*, 6073−6080.
(17) Mauk, M. R.; Mauk, A. G. *Eur. J. Biochem.* **1989**, *186*, 473−486.
(18) Drepper, F.; Dorlet, P.; Mathis, P. *Biochemistry* **1997**, *36*, 1418−1427.
(19) Muller, E.; Lapko, A.; Otto, A.; Muller, J. J.; Ruckpaul, K.; Heinemann, U. *Eur. J. Biochem.* **2001**, *268*, 1837−1843.
(20) Livingston, D. J.; McLachlan, S. J.; La Mar, G. N.; Brown, W. D. *J. Biol. Chem.* **1985**, *260*, 15699−15707.
(21) Grabarek, Z.; Gergely, J. *Anal. Biochem.* **1990**, *185*, 131−135.
(22) Miyazaki, G.; Morimoto, H.; Yun, K.; Park, S.; Nakagawa, A.; Minagawa, H.; Shibayama, N. *J. Mol. Biol.* **1999**, *292*, 1121−1136.
(23) Ye, S.; Shen, C.; Cotton, T. M.; Kostic, N. M. *J. Inorg. Biochem.* **1997**, *65*, 219−226.
(24) Furukawa, Y.; Ishimori, K.; Morishima, I. *Biochemistry* **2000**, *39*, 10996−11004.
(25) von Bodman, S. B.; Schuler, M. A.; Jollie, D. R.; Sligar, S. G. *Proc. Natl. Acad. Sci. U.S.A.* **1986**, *83*, 9443−9447.
(26) Teale, F. W. J. *Biochim. Biophys. Acta* **1959**, *35*, 543.
(27) Axup, A. W.; Albin, M.; Mayo, S. L.; Crutchley, R. J.; Gray, H. B. *J. Am. Chem. Soc.* **1988**, *110*, 435−439.
(28) Stayton, P. S.; Fisher, M. T.; Sligar, S. G. *J. Biol. Chem.* **1988**, *263*, 13544−13548.

to final concentrations of 5 and 2 mM, respectively.[21] After 3 h in the dark at 25 °C, a buffer of the reaction mixture was exchanged into 50 mM Na-P_i, pH 7.0 by using Centrifugal Filter Device and concentrated to 200 μL. The crude cross-linked product between ZnMb and Cytb_5 was eluted over a column (1.0 cm × 30 cm) of Superdex 75 fitted to a FPLC system, which was equilibrated with 50 mM Na-P_i, pH 7.0. The flow rate was 0.1 mL/min, and the elution was fractionated by 0.5 mL to separate the polymeric materials, 1:1 cross-linked ZnMb:Cytb_5 (CL-ZnMb/b_5), unreacted ZnMb, and Cytb_5 from reaction mixture. The cross-linking between ZnMb and Cytb_5 was confirmed by SDS-gel electrophoresis and MALDI-TOF mass spectrometry. Upon the sample preparation for the MALDI-TOF mass spectrometry, about 5 pmol of the proteins was mixed on the sample plate with 1 μL 3,5-dimethoxy-4-hydroxycinnamic acid in 30% acetonitrile containing 0.3% TFA, and the resultant spot was allowed to air-dry. The measurement conditions for the mass spectrometry were shown in detail in the "MALDI-TOF Mass Spectrometry" subsection.

The concentration of ZnMb was determined by using $\epsilon_{280} = 13.5$ mM^{-1} cm^{-1}, and the concentration of CL-ZnMb/b_5 in the sample was spectrometrically determined from the absorbance at 450 nm ($\epsilon_{450} =$ 12.12 mM^{-1} cm^{-1}), where ZnMb has little absorbance.

The Peptide Mapping of CL-ZnMb/b_5. The proteins were digested by trypsin as reported by Park et al.[30] with minor modification. Before the tryptic digestion, heme or ZnMP was extracted from the proteins by the acid-butanone procedure, to promote the hydrolysis of the hemoproteins by trypsin. Briefly, 3 μL of 1 N HCl was added to 50 μL of ca. 50 μM protein solutions dissolved in water, and an equivolume of 2-butanone was further added. After the centrifugation, the aqueous solutions were transferred to the other eppendorf microtubes containing 450 μL of 50 mM ammonium bicarbonate to make the final protein concentration of 1−5 μM. These protein solutions were thermally denatured by the incubation at 90 °C for 20 min. Following the incubation, the proteins were transferred to an ice−water bath to quench the denaturation process. The thermally denatured proteins were enzymatically digested with trypsin (Sigma Chemical Co. sequencing grade) at 37 °C for 3 h. The concentration of trypsin was 25:1 (wt of proteins/wt of trypsin) for all experiments. The digested peptides were analyzed by the MALDI-TOF mass spectrometry. On the sample plate, approximately 5 pmol of digested proteins (~ 1 μL) was mixed with 1 μL of α-cyanno-4-hydroxycinnamic acid in 30% acetonitrile containing 0.01% TFA, and allowed to air-dry. MS−FIT from University of California (San Francisco, CA) was used to identify the digest fragments and to estimate extent of the digestion.

MALDI-TOF Mass Spectrometry. All MALDI-TOF mass spectra were acquired using a PerSpective Biosystems Voyager DE PRO−SD equipped with a pulse nitrogen laser (337 nm), and obtained by using delayed extraction in the linear mode. Total ion acceleration voltage was 20 kV, and the grid voltage was 19.0 (for peptides) or 18.6 kV (for proteins). The delay time between laser pulse and voltage pulsing in the extraction plate was 125 (for peptides) or 375 ns (for proteins). Signals from 100 laser shots were averaged to increase the S/N ratio of each mass spectrum. The mass spectra of the digested peptides were calibrated using des-Arg^1-bradykinin (m/z = 904.4681), angiotensin I (m/z = 1296.6853), Glu^1-fibrinopeptide B (m/z = 1570.6774) and neurotensin (m/z = 1672.9175). In the case of ZnMb, Cytb_5 and CL-ZnMb/b_5 proteins, the mass spectra were calibrated by insulin (m/z = 5734.59), thioredoxin (m/z = 11674.48) and apomyoglobin (m/z = 16952.56).

Laser Flash Photolysis. As shown in Scheme 1, a laser pulse at 532 nm initiates the ET reaction from the triplet excited state of ZnMb

Scheme 1

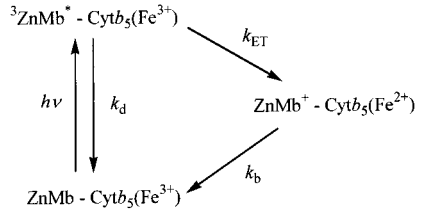

(^{3}ZnMb*) to ferric Cytb_5. The strong reducing ability of ^{3}ZnMb* ($E° \approx -0.8$ eV)[31] allows the transfer of one electron to ferric Cytb_5 ($E° \approx 5$ meV).[32] After the "forward" ET from ^{3}ZnMb* to ferric Cytb_5, the cation radical state of ZnMb (ZnMb$^+$) and ferrous Cytb_5 was formed. Since ZnMb$^+$ has much higher reduction potential (0.98 eV)[31] than Cytb_5, the "back" ET allows ferrous Cytb_5 and ZnMb$^+$ to return to the original states, ferric Cytb_5 and ZnMb, respectively. In this study, we examined the ET reactions between ZnMb and Cytb_5 by monitoring the absorbance change of ^{3}ZnMb* at 475 nm,[12] where ^{3}ZnMb* is the dominant absorber.[34] The formation and decay of ferrous Cytb_5 was also checked by monitoring the absorbance change at 420 nm, the isosbestic point between ^{3}ZnMb* and ZnMb with the significant absorbance of ferrous Cytb_5.

In the laser experiments, the dissolved oxygen in the sample must be removed, since ^{3}ZnMb* is also quenched by O_2.[35,36] To keep anaerobicity, we have tested the enzymatic deoxygenation using 10 mM D-glucose, 115 μg/mL glucose oxidase and 30 μg/mL catalase, as performed by Nocek et al.[12] In this method, however, the decay of ^{3}ZnMb* was severely accelerated (ca. 5-fold faster) after the sample was left for 30−60 min probably due to the production of protons by this enzymatic deoxygenation reaction. To eliminate this undesired effect on the decay acceleration, we did not use the above enzymatic deoxygenation, and instead the samples in the vacuum cell were vigorously degassed and purged with Ar gas by using vacuum line. Under this condition, the decay of ^{3}ZnMb* was virtually unchanged even after a day.

The second harmonic (532 nm) of a Q-switched Nd:YAG laser provided photolysis pulses with a half peak duration of 10 ns. The monitoring beam was generated by a xenon lamp (150 W), and focused on the sample cell at the right angle of the excitation source. The transmitted light went through the 0.2 mm-width slit, and was detected by a photomultiplier that is attached on a monochromator, UNISOKU USP-501. A two-channel oscilloscope (TDS520) was used to digitize and accumulate the signals that were transferred to a Gateway SELECT 1100 personal computer for the further analysis. Temperature was controlled by using a circulating water bath (±0.2 °C). The solution condition for the laser measurements was 1 mM Na-P_i, pH 6.0. To evaluate the ionic strength effects on the kinetics, we added 1 mM Na-P_i, 1M NaCl, pH 6.0 to the solution and increased the solution ionic strength up to 200 mM.

Brownian Dynamics Simulation. Brownian dynamics simulations of the encounter complex formed by ZnMb and Cytb_5 were performed

(29) The distribution of the binding conformations could be dependent upon the ionic strength of solution. Because approximately 50 mM of ionic strength would be the upper limit for the successful cross-linking by EDC (ref 17), we have also attempted the cross-linking under 1 mM Na-P_i, 50 mM NaCl, and pH 6.0. No differences were detected in the ET kinetics between 1 and 50 mM ionic strength, and the distribution of the binding conformations would be independent of the ionic strength below 50 mM.

(30) Park, Z.; Russell, D. H. *Anal. Chem.* **2000**, *72*, 2667−2670.
(31) Cowan, J. A.; Gray, H. B. *Inorg. Chem.* **1989**, *28*, 2074−2078.
(32) Reid, L. S.; Mauk, M. R.; Mauk, A. G. *J. Am. Chem. Soc.* **1984**, *106*, 2182−2185.
(33) Elias, H.; Chou, M. H.; Winkler, J. R. *J. Am. Chem. Soc.* **1988**, *110*, 429−434.
(34) According to Scheme 1, ferric and ferrous Cytb_5, ^{3}ZnMb*, ZnMb, and ZnMb$^+$ can contribute to the absorbance change in the present photoinduced ET reaction. The transient absorption spectroscopy (data not shown) have indicated that the difference in the molar extinction coefficient between ^{3}ZnMb* and ZnMb was about 20 mM^{-1} cm^{-1} at 475 nm. In contrast, the static difference spectrum (data not shown) between ferrous and ferric Cytb_5 showed much smaller contribution to the absorbance changes at 475 nm; $\Delta\epsilon$(ferrous − ferric) = −3.5 mM^{-1} cm^{-1}. Although ZnMb$^+$ is not stable enough to acquire its static spectrum, previous studies have implied that the absorption change to form the cation radical in Zn-substituted hemoproteins is less significant at 475 nm; for example, $\Delta\epsilon$(cation radical − ground state) = 4 mM^{-1} cm^{-1} in Zn-substituted cytochrome *c* (ref 33).
(35) Barboy, N.; Feitelson, J. *Biochemistry* **1987**, *26*, 3240−3244.
(36) Furukawa, Y.; Ishimori, K.; Morishima, I. *J. Phys. Chem. B* **2000**, *104*, 1817−1825.

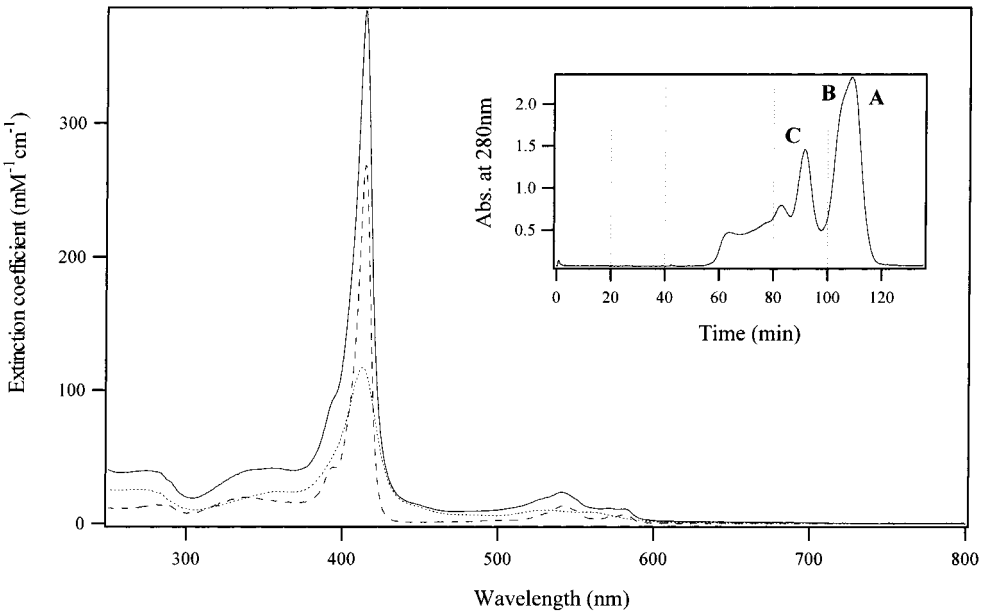

Figure 1. Electronic absorption spectra of CL-ZnMb/b_5 (solid line), ZnMb (broken line), and Cytb_5 (dotted line). The sum of the spectra of ZnMb and Cytb_5 is virtually the same with the spectrum of CL-ZnMb/b_5. Solution condition is 1 mM Na-P_i, pH 6.0. (Inset) The elution profile of the cross-linked reaction mixture between ZnMb and Cytb_5 by the gel filtration column, Superdex 75. The sample was eluted in 50 mM Na-P_i, pH 7.0, 4 °C. The flow rate was 0.1 mL/min.

with the MacroDox ver. 3.2.1, which was developed by Northrup et al.,[37] with the SGI O_2 workstation. The details of the algorithm used in this package are given in Northrup et al.[38] For the coordinates of Cytb_5, we used the solution NMR minimized average structure of oxidized rat microsomal Cytb_5 (1AW3)[39] by deleting the coordinates for hydrogen atoms. The X-ray crystal structure of horse heart recombinant myoglobin (1WLA)[40] was used to represent the structure of ZnMb. The encounter complexes formed by ZnMb and Cytb_5 were simulated as the 5000−10000 Brownian dynamics docking trajectories.

In our execution of the Brownian dynamics algorithm for this work, MacroDox declares a trajectories successful if the two reactive atoms in the proteins come within the reaction distance, which are set in the course of the simulations, before the mobile ligand (Cytb_5 in this study) passes outside a predefined outer escape radius, 200 Å.[38] For the simulation[41] of the encounter complexes formed between ZnMb and Cytb_5, we selected atoms near the center of mass in ZnMb (the carbon atom at the periphery of the porphyrin ring, CBB) and Cytb_5 (the α carbon atom of Val23) as the reactive atoms, and the reaction distance was set to 48 Å, which is the sum of the maximum distances from the center of mass in ZnMb (24 Å) and Cytb_5 (24 Å). In each simulated complex, the Fe−Fe distance was monitored to evaluate the ET reactivity. We also set the mutual angle between the heme planes as within 90 degrees, and therefore only the distance between the centers of mass in the two proteins is a factor for the protein−protein docking trajectories.

Results

Cross-Linking between ZnMb and Cytb_5. The elution profile obtained from passing the cross-linking reaction mixture over Superdex 75 gel filtration column is shown in the inset of Figure 1. The SDS-gel electrophoresis (data not shown) of each fraction proves that unreacted ZnMb eluted at peak A with the shoulder B containing unreacted Cytb_5, and CL-ZnMb/b_5 (peak C) eluted faster than unreacted ZnMb or Cytb_5. The fractions eluted faster than peak C (the elution at 60−85 min in the inset of Figure 1) had polymeric cross-linked ZnMb/Cytb_5 products, which were confirmed by the SDS-gel electrophoresis. The successful cross-linking between ZnMb and Cytb_5 can also be supported by the electronic absorption spectrum. Figure 1 shows the absorption spectrum of the fraction eluted at 90−95 min (peak C in the inset of Figure 1). The spectrum of peak C (the solid line in Figure 1) can be well simulated by equally summing up the spectra of ZnMb and ferric Cytb_5 (the broken and dotted spectra in Figure 1), and the homodimer such as ZnMb−ZnMb and Cytb_5−Cytb_5 was not able to reproduce the observed absorption spectrum of CL-ZnMb/b_5. These results suggest that ZnMb was cross-linked with Cytb_5 at the 1:1 ratio.[42] For further experiments, the fraction eluted from 90 to 95 min in the chromatogram (the inset of Figure 1) was used as CL-ZnMb/b_5.

We further confirmed the cross-linking between ZnMb and Cytb_5 by utilizing the MALDI-TOF mass spectrometry. The mass spectra of ZnMb and Cytb_5 showed signals at $m/z = 16968$ and 11226, respectively (Figure 2, A and B). These m/z values are in good accordance with those predicted from the amino acid sequence of ZnMb ($m/z = 16951$) and Cytb_5 ($m/z = 11210$) without ZnMP and heme, respectively, and the peak at around 22500 in the mass spectrum of Cytb_5 (Figure 2B) would correspond to dimeric Cytb_5. These mass spectra of the hemoproteins also indicated that heme or ZnMP was dissociated from the proteins in the course of the mass spectrometric

(37) Northrup, S. H. Software for the Prediction of Macromolecular Interaction; MacroDox v.3.2.1; Tennessee Technological University, Cookeville, TN, 1999.
(38) Northrup, S. H.; Boles, J. O.; Reynolds, J. C. L. *J. Phys. Chem.* **1987**, *91*, 5991−5998.
(39) Arnesano, F.; Banci, L.; Bertini, I.; Felli, I. C. *Biochemistry* **1998**, *37*, 173−184.
(40) Maurus, R.; Overall, C. M.; Bogumil, R.; Luo, Y.; Mauk, A. G.; Smith, M.; Brayer, G. D. *Biochim. Biophys. Acta* **1997**, *1341*, 1−13.
(41) Pearson, D. C.; Gross, E. L. *Biophys. J.* **1998**, *75*, 2698−2711.
(42) The SDS-gel electrophoresis (data not shown) showed the absence of the contamination of polymeric materials in the sample eluted from 90 to 95 min in the gel-filtration chromatogram. The contamination of free materials, ZnMb and Cytb_5, in the CL-ZnMb/b_5 sample was also not significant, because the electronic absorption spectrum of CL-ZnMb/b_5 can be well simulated with the 1:1 summation of ZnMb and Cytb_5 spectra and the observed kinetics in CL-ZnMb/b_5 was not dependent on the sample concentration (vide infra).

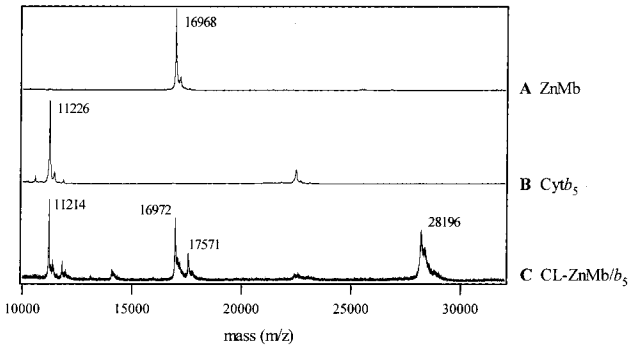

Figure 2. MALDI-TOF mass spectra of (A) ZnMb, (B) Cytb_5, and (C) CL-ZnMb/b_5. The matrix was 3,5-dimethoxy-4-hydroxycinnamic acid, and the spectra were averaged over 100 laser shots.

measurements. Figure 2C is the mass spectrum of CL-ZnMb/b_5 (peak C in the inset of Figure 1), and shows the signal at $m/z = 28196$, which was not observed in the mass spectrum of ZnMb or Cytb_5 alone, with the other peaks at $m/z = 11214$, 16972, and 17571. The observed m/z value, 28196, corresponds to the apo-form of CL-ZnMb/b_5, showing that one ZnMb molecule was cross-linked with one Cytb_5 by using the amino acid residues in ZnMb and Cytb_5.

Among the other peaks at 11214, 16972 and 17571, the first two m/z values, 11214 and 16972, could derive from the apo-forms of Cytb_5 and ZnMb, while the other peak at 17571 was not seen in the case of ZnMb or Cytb_5 and appears to correspond to the species having apo-Mb plus heme (calculated $m/z = 17567.5$). It is likely that the cross-link by EDC also occurred between the amino group in ZnMb and the heme propionates in Cytb_5.[20,43] Accordingly, the mass spectrometry of CL-ZnMb/b_5 confirms the successful cross-linking between ZnMb and Cytb_5, and the cross-linking between ZnMb and Cytb_5 is heterogeneous; the ϵ-amino group of ZnMb was cross-linked with the heme propionates in Cytb_5, or with the carboxyl group in Glu and/or Asp of Cytb_5.

Tryptic Peptide Mapping. To identify the cross-linking sites in CL-ZnMb/b_5, we attempted the peptide mapping by using the MALDI-TOF mass spectrometry. Figure 3 shows the mass spectra of the peptides of ZnMb (A), Cytb_5 (B), and CL-ZnMb/b_5 (C) digested by sequencing-grade trypsin. As summarized in Table 1, the observed mass peaks can be assigned to the tryptic digest peptides predicted by the MS-FIT program. For ZnMb, 14 digested fragments were detected, which corresponds to 92% coverage of the total amino acid sequence in ZnMb. In the case of Cytb_5, eight tryptic peptides were identified and cover 79% of the amino acid sequence.

On the basis of the tryptic peptide maps in ZnMb and Cytb_5 (Figure 3, A and B, and Table 1), we deduced the cross-linking site from the mass spectrum of the tryptic peptides in CL-ZnMb/b_5. In Figure 3C, we showed the tryptic peptide map of CL-ZnMb/b_5, and noticed that the peptides containing residues 48−56, 80−96, 79−96, 78−96, and 146−153 of ZnMb (the mass peaks indicated by arrows) were absent. The cross-linking by EDC alters the properties of the Lys, Glu, and Asp residues by the formation of an amide bond between ϵ-amino group of Lys and carboxylate group of Glu or Asp.[21] Although Lys residues are the specific cleavage sites by trypsin, the Lys residue at the cross-linking site is not further recognized by trypsin due to the formation of the amide bond with Glu or Asp. Also the mass peaks of the peptides containing the Glu or the Asp residues that are cross-linked with the Lys residues will disappear from their original positions. It is, therefore, suggested that the surface Lys (Lys 50, 56, 78, 79, 87, 147) or carboxyl group of Glu (Glu 52, 54, 83, 85, 148) in these vanished peptides (Table 1) are the cross-linking sites on ZnMb with Cytb_5. The vanished peptides contain no Asp residues. In Figure 4A are shown these probable interaction residues of ZnMb with Cytb_5, which encompasses the hemisphere including the exposed ZnMP edge of ZnMb. Lys and Glu residues in the peptides shown above, the peak intensities (Table 1) of which are lost upon the

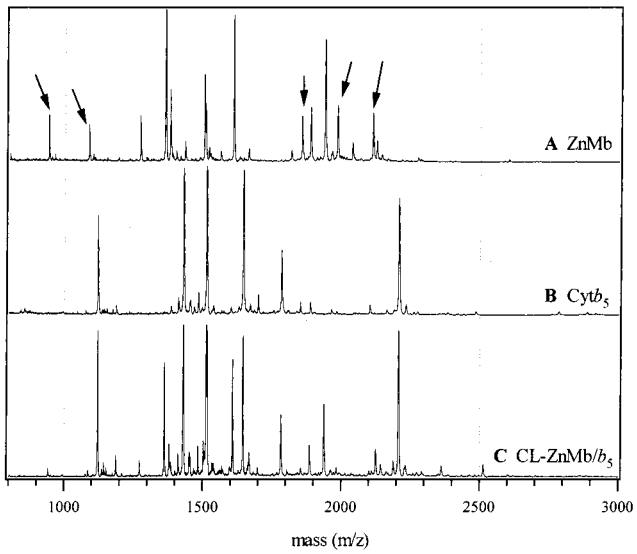

Figure 3. Tryptic peptide mapping analysis by the MALDI-TOF mass spectrometry. (A) ZnMb, (B) Cytb_5, and (C) CL-ZnMb/b_5. The arrows show the peptides that disappear or significantly reduce its peak intensity upon the cross-linking.

Table 1. Summary of the Tryptic Peptides Detected by MALDI-TOF Mass Spectrometry[a]

ZnMb			Cytb_5		
residue	calcd m/z	obsd m/z	residue	calcd m/z	obsd m/z
146−153	941.473	941.3	24−32	1120.626	1120.5
48−56	1086.561	1086.4	77−88	1428.712	1429.5
32−42	1271.663	1271.5	39−51	1511.749	1512.6
134−145	1360.758	1360.5	77−90	1643.839	1643.7
64−77	1378.842	1378.7	10−23	1781.907	1781.7
119−133	1502.669	1502.5	73−88	1885.965	1886.6
17−31	1606.855	1606.7	73−90	2101.092	2102.0
32−45	1661.853	1661.6	52−72	2205.928	2207.1
1−16	1815.902	1815.8			
80−96	1853.962	1854.7			
103−118	1885.022	1885.8			
32−47	1937.017	1937.7			
79−96	1982.057	1983.1			
78−96	2110.152	2110.9			

[a] The peptides shown in bold had diminished mass peaks upon the cross-linking.

(43) Although the mass peak at 16972 corresponds to the apo-form of ZnMb, it is unlikely that the CL-ZnMb/b_5 sample contains the unreacted ZnMb from the following reasons. The electronic absorption spectrum (Figure 1) and the disappearance of the specific ZnMb peptides in CL-ZnMb/b_5 (shown later, Figure 4) are consistent with the well separation of cross-linked product from the unreacted ZnMb. Also, the ET kinetics as mentioned later is independent of the concentration of the CL-ZnMb/b_5 sample, indicating that the CL-ZnMb/b_5 sample is almost free from the unreacted proteins. Nonetheless, a small peak at around $m/z = 11816$ might indicate the species of apo-Cytb_5 ($m/z = 11210$) linked with ZnMP ($m/z = 630.08$) via the amide bonds. In addition, it is plausible that the cross-link is possibly cleaved in several amounts of CL-ZnMb/b_5 during the measurements of the MALDI-TOF mass spectrum, resulting in the formation of apo-ZnMb.

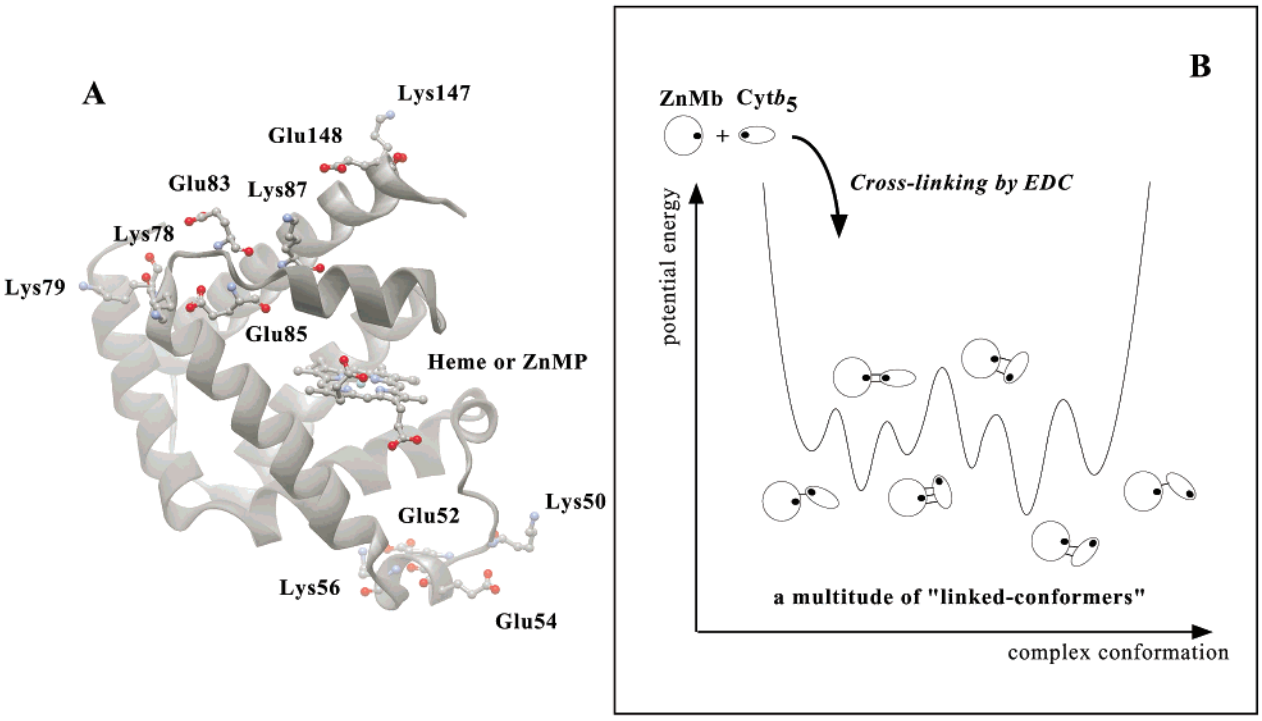

Figure 4. (A) Cross-linking sites on ZnMb estimated from the peptide mapping analysis. Lys and Glu residues in the peptides whose peak intensities disappear upon the cross-linking (Table 1) are shown in the "ball-and-stick" model and are most possible cross-linked sites. (B) The schematic representation on the "linked-conformers" formed by the cross-linking. The linked-conformers contain a multitude of protein−protein orientations as defined in the text. The solid black circles show ZnMP and heme in ZnMb and Cytb_5, respectively.

cross-linking, are shown in the ball-and-stick model and are the most possible cross-linked sites with Cytb_5. Such a broad interaction surface on ZnMb against Cytb_5 is consistent with the previous suggestions by Nocek et al.[12]

In contrast to the disappearance of some peptides in ZnMb, we were not able to find any peptides of Cytb_5 that are missing on the cross-linking with ZnMb. If the specific site(s) in Cytb_5 is used to form the complex with ZnMb, the mass peaks of some peptides including the interaction site(s) with ZnMb would disappear from its original position. In this study, however, the mass spectrum of CL-ZnMb/b_5 implies that the cross-linking of Cytb_5 with ZnMb does not occur at the single specific site; the cross-link with ZnMb occurs through its heme propionates (m/z = 17571 in Figure 2C) or the amino acid residues (m/z = 28196 in Figure 2C). As previously reported in the cross-linking experiments between Cytb_5 and cytochrome *c*, which is also considered to have nonspecific interactions, Mauk and Mauk[17] have failed in the satisfactory resolution of the tryptic peptides in the cross-linked complex by using HPLC. Therefore, the failure to detect the vanished peptides in Cytb_5 upon the cross-linking implies that Cytb_5 has rather nonspecific interactions with ZnMb. Since the negative charges including carboxyl groups are widespread over the entire surface of Cytb_5,[39] it is likely that Cytb_5 can adopt many orientations against the partner protein through the electrostatic interactions, resulting in rather nonspecific cross-linking with ZnMb by EDC.

As suggested by the peptide-mapping experiments, therefore, the cross-linked sites on ZnMb with Cytb_5 spread over its hemisphere including ZnMP, while mostly the entire surface of Cytb_5 could be used for the cross-linking with ZnMb. In other words, such a nonspecific cross-linking in CL-ZnMb/b_5 is considered to trap the various ZnMb−Cytb_5 orientations formed between ZnMb and Cytb_5, as schematically shown in Figure 4B. Each of the cross-linked protein−protein orientations in CL-ZnMb/b_5 is called the "linked-conformer" in this study, and therefore CL-ZnMb/b_5 is composed of the assembly of these linked-conformers.

Electron-Transfer Kinetics. To reveal how a multitude of the linked-conformers contribute to the ET from ZnMb to Cytb_5, we examined the ET kinetics in CL-ZnMb/b_5. As described in the previous section, a lifetime of ^{3}ZnMb* generated by a laser pulse is shortened when the ET to the ferric heme in Cytb_5 occurs. On the basis of the ET scheme (Scheme 1), the observed decay rate, k_{obs}, of ^{3}ZnMb* can in principle be expressed as the following equation:

$$k_{obs} = k_d + k_{ET} \quad (1)$$

where k_d is the ^{3}ZnMb* intrinsic decay rate and k_{ET} is the ET rate from ^{3}ZnMb* to Cytb_5. To obtain the ET rate constant in CL-ZnMb/b_5, we at first characterized the intrinsic decay process by measuring the absorbance change at 475 nm in 3 μM ZnMb, where only ^{3}ZnMb* species absorbs (Figure 5A). The single-exponential function was adequate for fitting to the ^{3}ZnMb* decay, as exemplified by the random fitting residuals (upper panel of Figure 5A). The intrinsic decay rate constant, k_d, was 60 s^{-1}, which is in good agreement with that obtained in the previous studies.[31]

In contrast, the decay of ^{3}ZnMb* in CL-ZnMb/b_5 (Figure 5B) appears to consist of the two kinetic phases: the single-exponential process having the rate constant, 65 s^{-1} and the process which cannot be explained by single-exponential (faster than ~1 ms). The decay kinetics showed no dependence on the CL-ZnMb/b_5 concentration (1−10 μM) and the ionic strength in the solution (μ = 1−200 mM) (data not shown), indicating that the observed reaction is *intra*-molecular. The initial increase

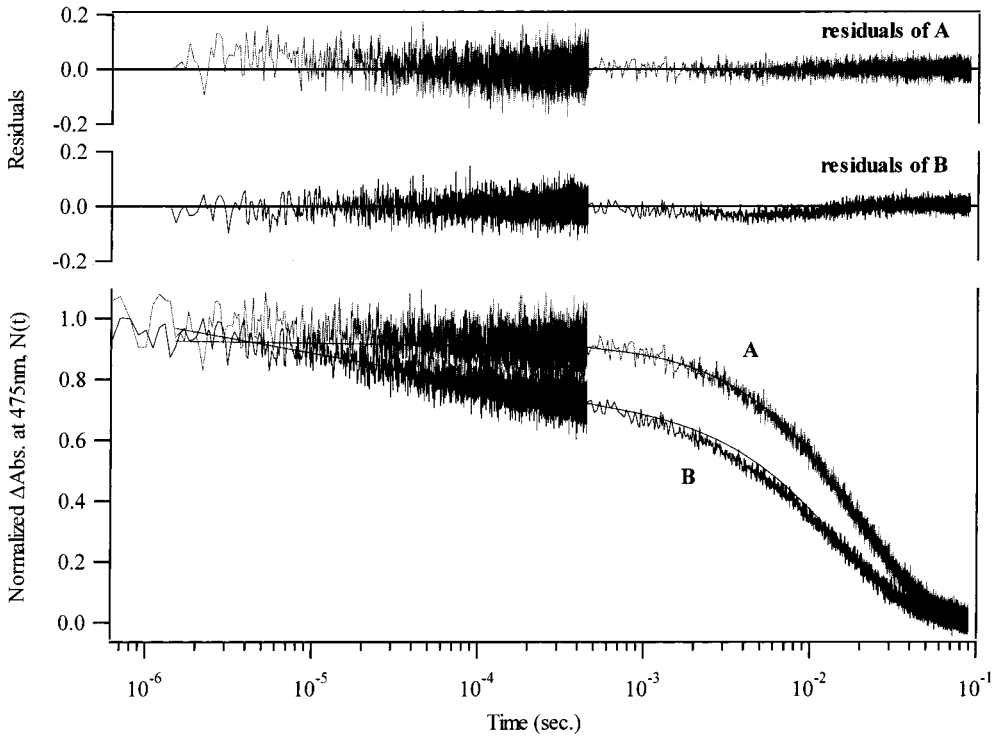

Figure 5. Normalized transient absorbance changes at 475 nm obtained after laser excitation of (A) 3 μM ZnMb and (B) 3 μM CL-ZnMb/b_5 in the log time scale. The residuals of the single-exponential fitting of the decay in ZnMb only (A) are shown on the top. The decay of CL-ZnMb/b_5 (B) can be well fitted by the function, $0.3(1 + 1.6 \times 10^{-5}t)^{-0.43} + 0.7\exp(-65t)$, as mentioned in the Discussion. The residuals to this fitting are also shown on the top (residuals of B). The sample conditions are 1 mM Na-P_i, pH 6.0, 293 K.

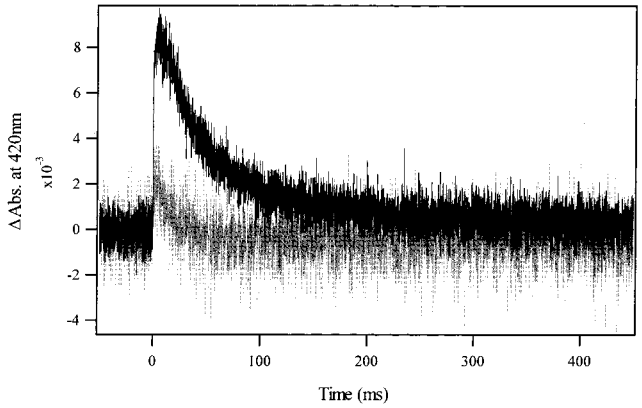

Figure 6. Absorbance changes at 420 nm, where the ZnMb/^{3}ZnMb* is the isosbestic and ferrous Cytb_5 mainly absorbs, after the laser excitation of 3 μM ZnMb (gray) and 3 μM CL-ZnMb/b_5 (black). The reaction condition is the same as that in Figure 5.

of the absorbance at 420 nm (Figure 6), where ferrous Cytb_5 absorbs, shows the formation of ferrous Cytb_5, which is consistent with the ET from ^{3}ZnMb* to ferric Cytb_5 in CL-ZnMb/b_5. We also confirmed that the titration of Cytb_5 over the 3 μM ZnMb solution accelerates the decay of ^{3}ZnMb*, but the decay process monitored at 475 nm remains the single exponential under 30−200 mM ionic strength (data not shown).[12,13] Therefore, the two kinetic phases observed in CL-ZnMb/b_5 are the characteristic consequences of the cross-linking.

In the ^{3}ZnMb* decay of CL-ZnMb/b_5 (Figure 5B), we at first notice that the rate constant, 65 s^{-1}, of the slower monophasic process is very similar to that of the ^{3}ZnMb* intrinsic decay, 60 s^{-1}. This single-exponential phase occupied about 70% of the total ^{3}ZnMb* decay. In the flash-photolysis method, the ET slower than the intrinsic decay of ^{3}ZnMb* is difficult to observe, since ^{3}ZnMb* decays dominantly through its intrinsic process (Scheme 1). In some linked-conformers (~70% of total conformers) of CL-ZnMb/b_5, therefore, the ET slower than k_d, 60 s^{-1}, might actually proceed, but we cannot observe such an unfavorable ET ($k_{ET} \lesssim 60$ s^{-1}) from ^{3}ZnMb* to Cytb_5.

Regarding the faster kinetic phase (10^{-6}−10^{-3} s in Figure 5B), which occupies about 30% of the total ^{3}ZnMb* decay, we attempted to fit this phase by exponential function, but the accurate number of the exponentials necessary for the adequate fitting appears not to be determined strictly. Alternatively, as represented in the double-logarithmic plot of the normalized absorbance change, $N(t)$, versus time, t, (Figure 7A), the absorbance change, log$N(t)$, of ^{3}ZnMb* in this phase (10^{-6}−10^{-3} s) is straight against the logarithmic time scale,[44] which follows the power law: $\log N(t) \propto -n\log t$. The power law (eq 2) has been frequently used for analysis of nonexponential processes[45,46]

$$N(t) = (1 + k_0 t)^{-n} \qquad (2)$$

The detailed analysis of this faster phase is discussed later in the Discussion.

Brownian Dynamics Simulation. To gain a further insight into the linked-conformers trapped by the cross-linking between ZnMb and Cytb_5, the protein-docking simulations using the Brownian dynamics (BD) algorithm were attempted. So far, in many studies, the BD docking calculations in redox proteins

(44) When the faster process is expressed as an exponential function, $N(t) = \exp(-kt)$, the shape of log $N(t)$ vs log t should not follow the straight line; $\log N(t) = -0.434\exp[2.30(\log k + \log t)]$.
(45) Austin, R. H.; Beeson, K. W.; Eisenstein, L.; Frauenfelder, H.; Gunsalus, I. C. *Biochemistry* **1975**, *14*, 5355−5373.
(46) Marden, M. C. *Eur. J. Biochem.* **1982**, *128*, 399−404.

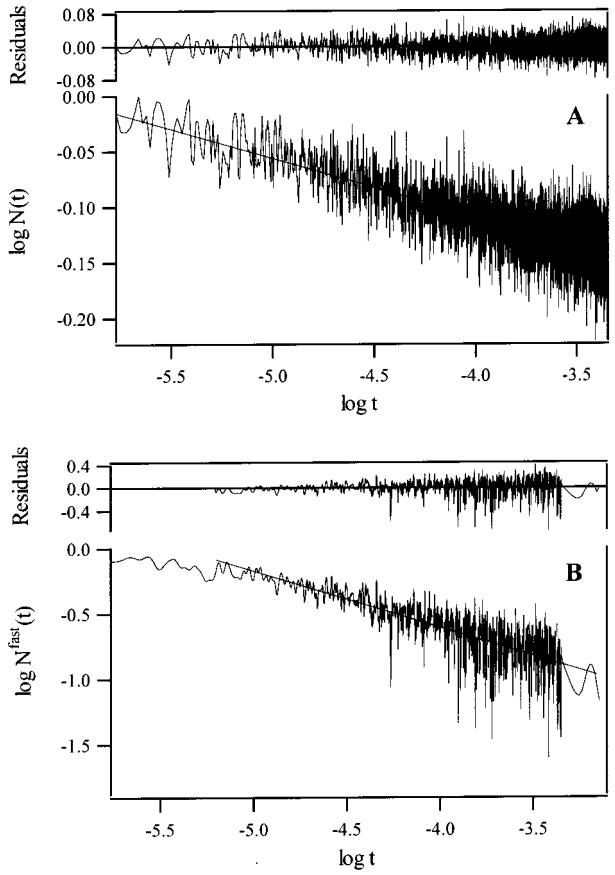

Figure 7. (A) Log−log plot of the normalized absorbance changes, $N(t)$, at 475 nm in CL-ZnMb/b_5 against time in the initial power-law region. The residuals of the linear fitting to this curve are shown on the top. (B) The log−log plot of $N^{fast}(t)$ of eq 6 against time in the initial power-law region, which was smoothed by least-squares polynomial smoothing in Igor Pro ver. 3.14. The residuals of the linear fitting to this curve are shown on the top.

have been designed to select complexes minimizing the distance at the ET active sites (for example, the zinc and iron atoms in ZnMb and Cytb_5, respectively) for the evaluation of the ET reactivity.[11,41,47] In this study, however, to reflect the cross-linking between ZnMb and Cytb_5 in the computer simulation, it would be desired that the simulation is independent of the distance between the ET active sites. As also suggested by Pearson and Gross,[41] the simulations by the minimization of the distance between the ET active sites do not really tell whether the two molecules preferentially form complexes at that reaction site. Therefore, we performed the BD docking by minimizing the distance between the atoms near the center of mass in the two proteins, which would represent purely the position of each protein molecule. Under these conditions, we could identify the complexes that are not ET-active in addition to complexes that are ET-active and realize the formation of a variety of the linked-conformers expected in CL-ZnMb/b_5. For evaluation of the ET reaction, the distance between the heme iron and the zinc ion in ZnMP, which would have some correlations with the donor−acceptor distance for the ET, was also monitored in the simulated complexes (see Discussion).

We at first performed the BD simulation of 10000 trajectories between ZnMb and Cytb_5 under 1 mM ionic strength, pH 6.0, and 293.15 K, and 7109 out of 10000 trajectories were obtained as the complexes successfully docked. In Figure 8 the solid

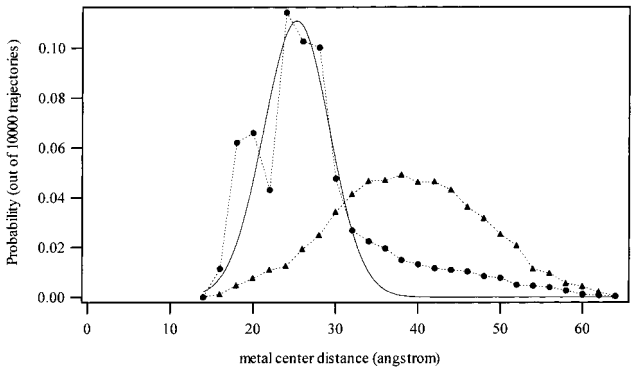

Figure 8. BD-simulated distribution of the metal-center distance in the encounter complexes formed between ZnMb and Cytb_5 (solid circles and broken line) under 1 mM and (solid triangles and broken line) 1 M ionic strength. All of the metal-center distances were rounded up to the nearest even number. For example, the number of complexes recorded at 20 Å represents all complexes with a metal-center distance, d, between 19 and 21 Å; $19 = d < 21$. The solid curve shows the Gaussian function fitted to the distribution of the metal-center distance from the BD simulation. The detailed condition is described in the Experimental Procedures section.

circles show the results of the BD simulations between ZnMb and Cytb_5 as a function of metal-center distance. In the course of the BD simulations, the significant probabilities to find the complexes with less than 30 Å of metal-center distance were suggested. The fraction of the complexes with the distance of <30 Å is 55% of the total trajectories, while that of the complexes having >30 Å distance is only 16%. Since the distribution is very broad and spans largely between 15 and 30 Å distance, the BD simulations also tell us that ZnMb binds Cytb_5 not at the single dominant site but with a multitude of mutual orientations between the proteins.

When the ionic strength in the simulation was raised to 1 M, where the random interactions would occur in the absence of electrostatic interactions, the distribution of the encounter complexes moves toward the larger distance [Figure 8 (solid triangle)] and the percentage of the occupation of the complex with <30 Å distance in the total trajectories is decreased to 12%. These results suggest that the electrostatic forces preferentially guide Cytb_5 to the binding sites on ZnMb with the <30 Å metal-center distance, although the binding between the proteins occurs not at the single site [Figure 8 (solid circle)] even under the low ionic strength (1 mM).

Discussion

As suggested by the peptide-mapping and the ET kinetics experiments, the cross-linking results in the entrapment of various protein orientations presumably formed in the encounter between ZnMb and Cytb_5, and contains a multitude of the "linked-conformers" (Figure 4B). As mentioned in the Introduction, the amino group (Lys) on the surface of protein is cross-linked by the reagent, EDC, with the electrostatically interacting carboxyl group (Glu or Asp) on the counterpart protein. Therefore, the present cross-linked product would not include the complexes stabilized by other interactions: for example, hydrogen bonding, hydrophobic interactions. In the ET reaction between ZnMb and Cytb_5, however, ZnMb has been proposed to bind Cytb_5 through the electrostatic interactions between Lys

(47) Northrup, S. H.; Thomasson, K. A.; Miller, C. M.; Barker, P. D.; Eltis, L. D.; Guillemette, J. G.; Inglis, S. C.; Mauk, A. G. *Biochemistry* **1993**, *32*, 6613−6623.

and Glu/Asp residues, and other interactions appear to be less important in the complex formation for ET.[12,20] Also, due to the nonspecific nature of the EDC-modification,[17] all of the surface Lys and Glu/Asp residues appear to be potent for the modification sites. It can, therefore, be considered that the complexes requisite for ET are successfully cross-linked by EDC.

To investigate the effects of these linked-conformers on the ET reaction between the proteins and quantitatively analyze the ET process in CL-ZnMb/b_5, we utilized the Marcus theory.[48] Previous studies [49] have revealed that the ET rate constants in proteins are dependent upon the distance between the redox centers (D−A distance), d_{ET}, the redox potential difference, $\Delta G°$, and the reorganization energy, λ. The dependencies of these determinants upon the ET rate are well explained by the Marcus equation in the following approximated form:[50]

$$k_{ET} = 10^{13} \exp[-\beta(d_{ET} - 3)] \exp\left[-\frac{(\Delta G^{o} + \lambda)^2}{4\lambda k_B T}\right] \quad (3)$$

where β is the distance decay factor, k_B is the Boltzmann factor, and T is the absolute temperature. In the ET reaction between ZnMb and Cytb_5, the protein−protein orientation in the complex influences the ET rate through the D−A distance, d_{ET}, and would have less impact on $\Delta G°$ and λ, because $\Delta G°$ and λ are determined mainly by the nature of the redox centers, ZnMP and heme.[48] For application of the Marcus equation, it is necessary to note that the observed kinetics is not due to the gated process by protein rearrangement, in which the rate constant is not dependent on the parameters in the Marcus equation, d, λ, and $\Delta G°$. Even if a reaction is not a true ET, its kinetic will apparently depend on the parameters in the Marcus theory, but fitting to the Marcus equation will yield unreasonable values of these parameters. In the case of the ET reactions gated by protein rearrangements, cross-linking abolishes the protein rearrangements requisite for the intracomplex ET reactions, and the rate constant in cross-linked sample is significantly deteriorated, which has been observed in the reaction between Zn-substituted cytochrome *c* (ZnCyt*c*) and plastocyanin (Pc).[51] In CL-ZnMb/b_5, however, the cross-linking did not decelerate the ET rate, which is in sharp contrast to the gated reaction between ZnCyt*c* and Pc. In the present CL-ZnMb/b_5 reactions, therefore, the analysis of the ET rates by the Marcus equation can afford the D−A distance, which provides us with the features of the protein−protein orientations in the linked-conformers trapped by the cross-linking.

ET Kinetics in the Cross-Linked Protein Complex. As shown in Figure 5B, CL-ZnMb/b_5 shows a complex decay kinetics of ^{3}ZnMb*: the initial power law process and the single-exponential decay process.[52] Since the power law phase in the ^{3}ZnMb* decay was significantly faster than its intrinsic decay

Scheme 2

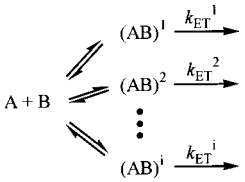

(Figure 5B), an electron is transferred to the Cytb_5 domain through this phase (eq 1). On the basis of a multitude of the linked-conformers between ZnMb and Cytb_5, which is suggested by the mass spectrometry and the peptide mapping analysis of CL-ZnMb/b_5, we analyzed the decay process of ^{3}ZnMb* in CL-ZnMb/b_5 as follows. A and B states in Scheme 2 mean the ZnMb and the Cytb_5 molecules, respectively, and each linked-conformer trapped in CL-ZnMb/b_5 is represented by (AB)^i.

In this scheme, the ET reaction in CL-ZnMb/b_5 can be expressed by the individual ET processes in the cross-linked complexes, (AB)^i, with the rate constant, $k_{ET}{}^i$. The decay of ^{3}ZnMb* in CL-ZnMb/b_5 can, therefore, be expressed by the sum of exponentials with rate constant, $k_{ET}{}^i$:[53]

$$N(t) = \sum_i h(k_{obs}{}^i) \exp(-k_{obs}{}^i t) \quad (4)$$

where $N(t)$ is the normalized absorbance change, $h(k_{obs}{}^i)$ is the fraction of the (AB)^i out of the total linked-conformers formed in CL-ZnMb/b_5, and $k_{obs}{}^i = k_{ET}{}^i + k_d$. Nevertheless, we cannot find the discrete number of exponentials explaining the power law process in the decay kinetics of CL-ZnMb/b_5, as mentioned in Results. In addition, the ET rate slower than the intrinsic decay rate, 60 s^{-1}, of ^{3}ZnMb* cannot be observed in this flash-photolysis method (Scheme 1). Instead, all of the CL-ZnMb/b_5 species having the ET rate slower than 60 s^{-1} show the single-exponential intrinsic decay of ^{3}ZnMb* with the rate constant, k_d, as exemplified in Figure 5B. We, therefore, attempted to describe the power law process (10^{-6}−10^{-3} s) as the spectrum of the ET rate constants and the plausible slower ET process (<60 s^{-1}) as the single-exponential intrinsic decay of ^{3}ZnMb* (eq 5).[53]

$$N(t) = A_1 \int_{k_d}^{\infty} h(k_{obs}) \exp(-k_{obs} t) dk_{obs} + A_2 \exp(-k_d t) \quad (5)$$

where A_1 and A_2 are the fractions of the power-law and the single-exponential process, respectively. As mentioned in the Results section, 70% of the total ^{3}ZnMb* decay follows the single-exponential phase, $A_2 \exp(-k_d t)$, in eq 5, while the other kinetic phase (about 30%), the power law phase, would correspond to the first term in eq 5, $A_1 \int_{k_d}^{\infty} h(k_{obs}) \exp(-k_{obs} t) dk_{obs}$. To evaluate $h(k_{obs})$, eq 5 can be rearranged into eq 6 as follows:

$$N^{fast}(t) = \frac{N(t) - A_2 \exp(-k_d t)}{A_1} = \int_{k_d}^{\infty} h(k_{obs}) \exp(-k_{obs} t) dk_{obs} \quad (6)$$

Since the observed rate constant, k_{obs}, in the power law phase is considered to be always larger than the intrinsic decay rate of ^{3}ZnMb*, k_d, (eq 1), the distribution function, $h(k_{obs})$, can be

(48) Marcus, R. A.; Sutin, N. *Biochim. Biophys. Acta* **1985**, *811*, 265−322.
(49) Winkler, J. R.; Gray, H. B. *Chem. Rev.* **1992**, *92*, 369−379.
(50) Page, C. C.; Moser, C. C.; Chen, X.; Dutton, P. L. *Nature* **1999**, *402*, 47−52.
(51) Zhou, J. S.; Kostic, N. M. *J. Am. Chem. Soc.* **1993**, *115*, 10796−10804.
(52) In the present study, the kinetics was examined separately in the faster (full scale, 500 μs) and the slower (full scale, 100 ms) time region, which are combined to illustrate the overall decay kinetics in the time region of 10^{-6}−10^{-1} s (trace B in Figure 5). In the combination procedure, the raw data on the slower time region were multiplied so as to smoothly match with the decay in the faster time region. The slight deviation from the random residuals shown in the slower time region of trace B in Figure 5 might be due to this combination procedure.
(53) Steinbach, P. J.; Chu, K.; Frauenfelder, H.; Johnson, J. B.; Lamb, D. C.; Nienhaus, G. U.; Sauke, T. B.; Young, R. D. *Biophys. J.* **1992**, *61*, 235−245.

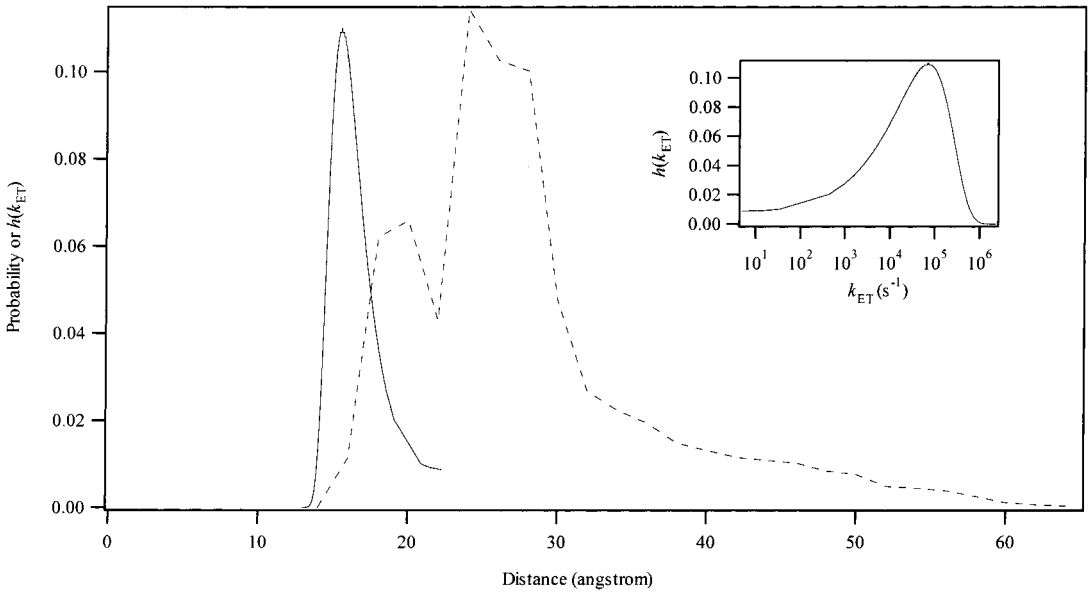

Figure 9. D−A distance distribution (solid line) predicted from the ET kinetics by using the Marcus equation (eq 3). The metal-center distance distribution (broken line) simulated from the BD docking between ZnMb and Cytb_5 is also shown. (Inset) The distribution of the ET rate constants estimated from the faster nonexponential ET process in CL-ZnMb/b_5 by using eq 9.

set to zero between 0 and k_d in k_{obs}, leading to the following equation.

$$N^{fast}(t) = \int_0^{k_d} h(k_{obs}) \exp(-k_{obs}t)\mathrm{d}k_{obs}\ (=0) + \int_{k_d}^{\infty} h(k_{obs}) \exp(-k_{obs}t)\mathrm{d}k_{obs} = \int_0^{\infty} h(k_{obs}) \exp(-k_{obs}t)dk_{obs} \quad (7)$$

The distribution function, $h(k_{obs})$, can, therefore, be expressed by the inversed Laplace transform of $N^{fast}(t)$.

$$L^{-1}N^{fast}(t) = h(k_{obs}) \quad (8)$$

According to eq 6, $N^{fast}(t)$ was calculated from the normalized absorbance change, $N(t)$, (Figure 5) by using the values of A_1, A_2, and k_d obtained from the initial fitting, 0.3, 0.7, and 65 s^{-1}, respectively. The power law fitting of $N^{fast}(t)$ afforded the k_0 and n values as 1.6×10^5 s^{-1}, 0.43, respectively, and the residuals of the linear fitting to $N^{fast}(t)$ were random (Figure 7B), indicating that the power law represents $N^{fast}(t)$ reasonably well. The substitution of the power law function for eq 8, therefore, gave an approximated form (eq 9) of the distribution function, $h(k_{obs})$.[53]

$$h(k_{obs}) = \ln 10 \frac{(k_{obs}/k_0)^n}{\Gamma(n)} \exp(-k_{obs}/k_0) \quad (9)$$

where Γ means the Gamma function. The peak of this distribution, given by $\mathrm{d}h(k_{obs})/\mathrm{d}k_{obs} = 0$, occurs at

$$k_{max} = nk_0 \quad (10)$$

and the value of n is related to the distribution width of the rate constants. By using the fitted values ($k_0 = 1.6 \times 10^5$ s^{-1}, $n = 0.43$) and eq 9, we can construct the approximate distribution profile of the rate constant with ca. 7.0×10^4 s^{-1} as the most probable k_{obs} in the power law phase. To obtain the distribution of the ET rate constant, $h(k_{ET})$, in CL-ZnMb/b_5, the intrinsic decay rate, k_d, was subtracted from the observed rate constant, k_{obs}, as shown in eq 1. The inset of Figure 9 shows the distribution profile of the ET rate constant, k_{ET}, obtained from the power law phase in CL-ZnMb/b_5.

From the distribution profile of the ET rate constant in CL-ZnMb/b_5 (inset of Figure 9), the D−A distance can be estimated from the Marcus equation (eq 3). In eq 3, the redox potential difference, $\Delta G°$, has been determined as much as −0.8 eV in the ET reaction between ZnMb and Cytb_5.[31,32] The reorganization energy, λ, and the distance decay factor, β, are set to 1.2 eV and 1.4 $Å^{-1}$, respectively, which have been encountered for many protein−protein ET reactions.[49] By using these values, the distribution of the ET rate constants in CL-ZnMb/b_5 can be converted into that of the D−A distance (solid line in Figure 9), and the linked-conformers trapped by the cross-linking would have a set of the ZnMb−Cytb_5 orientations represented by this distribution of the D−A distance.

Compared to the distance distribution obtained by the BD simulation (broken line in Figure 9), it is notable that the D−A distance in the analysis of the ET kinetics (solid line in Figure 9) is populated around the shorter distance (peak at 15 Å). Strictly, the D−A distance calculated from the ET rate constants is not the same with the Fe−Fe distance obtained by the BD simulation. Heme has the extended π-orbital over the porphyrin ring, and therefore the observed ET in CL-ZnMb/b_5 could occur through the heme edge not at the metal center. Since the porphyrin ring has an approximately 3 Å in its radius, the D−A distance would be at most ∼6 Å shorter than the distance between the metal centers. Even if the difference in the monitored atoms of heme is taken into account, the D−A distance from the ET kinetics tends to be shorter than the metal-center distance by the BD simulations.

As mentioned previously, we could not detect the ET slower than the ^{3}ZnMb* intrinsic decay rate, 60 s^{-1}, which corresponds to the D−A distance larger than 20 Å (eq 3). The cross-linked complexes having > 20 Å D−A distance are, therefore, not included in the distribution profile obtained from the analysis of the power law phase (solid line in Figure 9). Nevertheless,

the single-exponential process with 65 s^{-1} occupied about 70% of the total decay of ^{3}ZnMb* in CL-ZnMb/b_5, implying that the major protein−protein orientations trapped by the cross-linking have > 20 Å D−A distance with the inefficient ET reactions (<60 s^{-1}). In addition, the majority of the linked-conformers with >20 Å D−A distance (~70%) is consistent with the results of the BD simulation (solid circles in Figure 8). Accordingly, the D−A distance in the *major* cross-linked complexes (~70% of the total complexes) would be too long (>20 Å) to show the facile ET between ZnMb and Cytb_5 domains, while an electron is transferred via the formation of the *minor* complexes having the D−A distance between about 13−20 Å (~30% of the total complexes, solid line in Figure 9).

The Formulation of the ET Reaction with the Multiple Protein Orientations. Since the cross-linked complex is considered to trap the encounter complexes formed between ZnMb and Cytb_5, it is suggested that ZnMb can form a variety of encounter complexes with Cytb_5. On the basis of the results in CL-ZnMb/b_5 discussed above, therefore, the following picture on the ET reaction in the *mixture* of the ZnMb and the Cytb_5 molecules can be considered. A ZnMb molecule would encounter Cytb_5 mainly in the condition of D−A distance larger than ~20 Å, which cannot efficiently transfer an electron, resulting in the decay through the intrinsic process. Through the successive formation of various encounter complexes, however, smaller sets (presumably ~30% based on the ET kinetics of CL-ZnMb/b_5) of ZnMb−Cytb_5 complexes in the solution can achieve the shorter D−A distance around 13−20 Å, and, in those encounter complexes, the facile ET occurs.

To reveal the contribution of this minor encounter complex to the overall bimolecular ET reaction, the equation for the ET reaction within the distributed D−A distance was examined in this section. As previously reported,[12] the rapid-exchange limit holds good at the bimolecular ET reaction between ZnMb and Cytb_5 without the cross-linking. That is, the encounter complex formation and dissociation are faster than the *intra*-complex ET reaction rate, k_{ET}^i, in Scheme 2. Unlike the nonexponential kinetics seen in CL-ZnMb/b_5, therefore, ^{3}ZnMb* in the *mixture* with Cytb_5 decays exponentially with the apparent second-order ET rate constant, k_{app}, given by[13]

$$k_{app} = K_a^{all} \sum_i f^i k_{ET}^{\ i} \tag{11}$$

where K_a^{all} is the overall association constant and f^i is the fraction of the complex having the *intra*-complex ET rate constant, k_{ET}^i. According to this equation, various encounter complexes will contribute to the apparent bimolecular ET rate, k_{app}, but it is difficult to obtain the distribution of the encounter complex, f^i, and the *intra*-complex ET rate, k_{ET}^i, from the experimental values of k_{app}.

As discussed in the ET kinetics of CL-ZnMb/b_5, however, the interprotein ET reaction under the multiple protein−protein orientations can be explained by the distribution of the D−A distance. In eq 11, therefore, we are allowed to apply the Marcus equation to replace the fraction of the complex, f^i, by the distribution of the D−A distance, $g(d_{ET}^{\ i})$:

$$k_{app} = K_a^{all} \sum_i g(d_{ET}^{\ i}) A \exp(-\beta d_{ET}^{\ i}) \tag{12}$$

where $g(d_{ET}^{\ i})$ is the fraction of the complex having the D−A distance, d_{ET}^i, and A is defined by $A = 10^{13} \exp(3\beta) \exp[-(\Delta G^o + \lambda)^2/4\lambda k_B T]$. In eq 12, we assume the simple exponential distance dependence of ET rates. Strictly, protein ET reaction is also dependent on its electron pathway,[49] which is difficult to be analyzed with sufficient precision in the present data. While $g(d_{ET}^{\ i})$ also depends on the protein structure or the electrostatic characters of the protein surface, we assume, on the basis of the ET kinetics in CL-ZnMb/b_5 and the BD simulation (Figures 8 and 9), that $g(d_{ET}^{\ i})$ has the Gaussian distribution with the most probable distance, $\overline{d_{ET}}$, and the width parameter, σ, (eq 13).

$$g(d_{ET}) = \frac{1}{\sigma\sqrt{2\pi}} \exp\left[-\frac{(d_{ET} - \overline{d_{ET}})^2}{2\sigma^2}\right] \tag{13}$$

Since the compilation of the docking trajectories in the BD simulation of this study is independent of their potential energy (stability), the distribution of the metal-center distance, $g(d_{ET}^{\ i})$, estimated from the BD simulations, need not to be the same with that of the encounter complex stability, f^i. Accordingly, it has to be kept in mind that the application of the results of the BD docking through the Gaussian distribution function is a rough approximation for the evaluation of the bimolecular ET rate (eq 12). As shown in Figure 8, the distance simulated by the BD docking can well be reproduced by the Gaussian distribution: $\overline{d_{ET}}$ and σ are 25.2 and 4 Å, respectively (solid curve). By substituting eq 12 for eq 13, we obtained the equation for the apparent bimolecular ET rate in a variety of the encounter complexes, of which the D−A distance has the range from d_1 to d_2.

$$\begin{aligned} k_{app} &= \frac{AK_a^{all}}{\sigma\sqrt{2\pi}} \int_{d_1}^{d_2} \exp\left[-\frac{(d_{ET} - \overline{d_{ET}})^2 + 2\beta\sigma^2 d_{ET}}{2\sigma^2}\right] dd_{ET} \\ &= K_a^{all} A \exp(-\beta\overline{d_{ET}}) \left\{ \frac{\exp\left(\frac{\beta^2\sigma^2}{2}\right)}{\sigma\sqrt{2\pi}} \times \right. \\ &\qquad \left. \int_{d_1}^{d_2} \exp\left(-\frac{(d_{ET} - (\overline{d_{ET}} - \beta\sigma^2))^2}{2\sigma^2}\right) dd_{ET} \right\} \end{aligned} \tag{14}$$

In this equation, the first term, $K_a^{all} A \exp(-\beta\overline{d_{ET}})$, means the bimolecular ET rate constants at the D−A distance, $\overline{d_{ET}}$, and is constant under the distribution parameters, $\overline{d_{ET}}$ and σ. On the contrary, the remaining term in the brace, "orientation factor" ($F_{ori}(d_1, d_2)$) called in this study, depends on the range of the D−A distance, d_1 and d_2.

$$\begin{aligned} F_{ori}(d_1,d_2) &= \frac{\exp\left(\frac{\beta^2\sigma^2}{2}\right)}{\sigma\sqrt{2\pi}} \times \\ &\qquad \int_{d_1}^{d_2} \exp\left(-\frac{(d_{ET} - (\overline{d_{ET}} - \beta\sigma^2))^2}{2\sigma^2}\right) dd_{ET} \end{aligned} \tag{15}$$

As discussed previously, the analysis of the decay kinetics in CL-ZnMb/b_5 suggested that the facile ET occurs through the complexes with the D−A distance approximately between 13

and 20 Å. The ET rate slower than the ^{3}ZnMb* intrinsic decay rate, 60 s^{-1}, was also considered with the D−A distance larger than 20 Å. In the calculation of the orientation factor in eq 14, therefore, we call the complexes with the D−A distance smaller than 20 Å as "efficient ET complexes", while the other complexes (20−40 Å D−A distance) are termed as "inefficient ET complexes". In the Gaussian distribution function ($\overline{d_{ET}}$ = 25.2 Å, σ = 4 in eq 13) describing the results of the BD simulation (Figure 8), the efficient ET complexes are set to be less populated, and its occupancy in the total simulated encounter complexes is only 10%. On the other hand, 90% of the total encounters between the proteins result in the >20 Å D−A distance.

Under such a condition mentioned above (the complexes with 13−40 Å D−A distance) and with the value of 1.4 Å^{-1} for β,[49] the orientation factor in the efficient ET complexes (13−20 Å D−A distance, F_{ori}(13, 20)) is 3 × 10^4, while the inefficient ET complexes (20−40 Å D−A distance) have significantly smaller orientation factor (F_{ori}(20, 40)), 4 × 10^1 (eq 14). In addition, the apparent bimolecular ET rate constant, eq 14, can be expressed as the sum of the contributions from both of the efficient and the inefficient ET complexes (eq 16).

$$k_{app} = \{F_{ori}(13,20) + F_{ori}(20,40)\}\cdot K_a^{all}\cdot A \exp(-\beta\overline{d_{ET}}) \quad (F_{ori}(13,20) = 3 \times 10^4, \quad F_{ori}(20,40) = 4 \times 10^1) \quad (16)$$

As obviously seen in eq 16, the contribution of the efficient ET complexes to the bimolecular ET rate, $F_{ori}(13,20)\cdot K_a^{all}A \exp(-\beta\overline{d_{ET}})$, is 10^3-fold more significant than that of the inefficient ET complex, $F_{ori}(20,40)\cdot K_a^{all}A \exp(-\beta\overline{d_{ET}})$, despite the larger population of the inefficient ET complex (∼90% of the total simulated complexes, Figure 8). This result means that small fractions of the efficient ET complexes can determine the overall bimolecular ET reaction, even when the most probable binding site is too remote from the ET active site (25.2 Å in this case) to efficiently transfer an electron.

In summary, this study demonstrates that in solution ZnMb and Cytb_5 can form the encounter complexes with a multitude of the D−A distances. Although the encounter complexes with the shorter D−A distance (<20 Å) and the high ET reactivity are less populated, the bimolecular ET reaction would be regulated by this small fraction of the protein−protein orientations.

Acknowledgment. This work was supported by a grant from Ministry of Education, Science, Culture, and Sports (to I. M., No.12002008). Y. F. was supported by Research Fellowships of Japan Society for the Promotion of Science for Young Scientists. We are grateful to Prof. Stephen G. Sligar (University of Illinois) for a gift of the expression vector of the rat hepatic cytochrome b_5 gene. We are also obliged to Dr. Satoshi Takahashi (Kyoto University) for the fruitful discussion.

JA0171916